nature neuroscience

Vascular niche factor PEDF modulates Notch-dependent stemness in the adult subependymal zone

Celia Andreu-Agulló[1,2], José Manuel Morante-Redolat[1], Ana C Delgado[1] & Isabel Fariñas[1]

We sought to address the fundamental question of how stem cell microenvironments can regulate self-renewal. We found that Notch was active in astroglia-like neural stem cells (NSCs), but not in transit-amplifying progenitors of the murine subependymal zone, and that the level of Notch transcriptional activity correlated with self-renewal and multipotency. Moreover, dividing NSCs appeared to balance renewal with commitment via controlled segregation of Notch activity, leading to biased expression of known (*Hes1*) and previously unknown (*Egfr*) Notch target genes in daughter cells. Pigment epithelium–derived factor (PEDF) enhanced Notch-dependent transcription in cells with low Notch signaling, thereby subverting the output of an asymmetrical division to the production of two highly self-renewing cells. Mechanistically, PEDF induced a non-canonical activation of the NF-κB pathway, leading to the dismissal of the transcriptional co-repressor N-CoR from specific Notch-responsive promoters. Our data provide a basis for stemness regulation in vascular niches and indicate that Notch and PEDF cooperate to regulate self-renewal.

Asymmetric division preserves adult stem cell pools while ensuring tissue renewal. However, individual stem cells appear to be capable of undergoing symmetric divisions to generate two stem (expansionary self-renewing divisions) or two committed (differentiative divisions) cells, and the balance between these division modes probably regulates the dynamics of stem-cell reservoirs[1]. Some intrinsic determinants are known to regulate division mode, but stem cells can respond to excessive cellular demand after injury, suggesting that their self-renewing behavior can be modulated by external signals[1,2]. In the specialized stem-cell microenvironments, vascular elements appear to be important for the regulation of stem cell self-renewal versus commitment both under normal and pathological conditions, but the signaling pathways involved are still under investigation[3].

In the subependymal zone (SEZ) of the adult mammalian brain, persistent and relatively quiescent astroglia-like neural stem cells (NSCs) support life-long production of neuroblasts and oligodendrocytes that are destined to go to the olfactory bulb and the corpus callosum, respectively, through the production of fast-dividing transit-amplifying progenitors (TAPs)[3,4]. Clusters of neurogenic progenitors intimately apposed to brain capillaries suggest that vascular elements are an essential feature of adult NSC microenvironments[5–7] and several endothelium-derived factors are known to regulate proliferation and/or survival of neural progenitors[3]. Indirect coculture experiments have shown that capillaries are also a source of NSC self-renewal–promoting molecules[8] and we have recently reported that PEDF (also known as Serpin-F1) is, at least in part, responsible for these effects[9]. The secreted glycoprotein PEDF can promote tumor cell differentiation and neuronal survival and is a highly potent anti-angiogenic factor[10], in addition to acting as an endogenous SEZ niche factor that promotes NSC expansionary divisions[9]. Although a molecule with phospholipase activity can seemingly bind PEDF in some cells[11], the identity of the receptor(s) that could mediate the various PEDF effects, including those relating to NSC self-renewal, remains unknown.

Notch signaling is important for the maintenance of stem cells in various niches[12,13] and, notably, NSCs treated with PEDF have upregulated expression of Notch-downstream effectors Hes1 and 5 of the HES family of basic helix-loop-helix transcription factors[8,9]. Activation of Notch (1–4 in mammals) receptors by membrane-bound ligands (Jagged1/2 or Delta 1–4) is followed by regulated cleavage by a presenilin–γ-secretase complex. The generated intracellular domain of Notch (NICD) then moves to the nucleus, where it binds the repressor C promoter–binding factor 1 (CBF1, also known as RBP-J and CSL) to initiate transcription of genes of the *Hes* and *Herp* families[13,14]. HES transcription factors negatively regulate the expression of pro-neurogenic genes and Notch signaling therefore enhances self-renewal by antagonizing differentiation, although it can also regulate proliferation and survival[15–18]. Studies in transgenic Notch activity–reporter (TNR) mice have shown that high CBF1 activity distinguishes stem cells from committed progenitors[2,19,20] and loss-of-function experiments have demonstrated that downregulation of Notch activity is required for the transition from radial glia/astroglia-like cells to committed progenitors[20,21]. Putative differences in Notch activity levels in SEZ cells are unknown, but Notch activity is required to sustain NSC maintenance in this niche[15–17].

Here, we sought to investigate potential interactions of PEDF with the Notch pathway. We found that subependymal cells that had reporter activation in TNR mice were contained in the population

[1]Departamento de Biología Celular and CIBER en Enfermedades Neurodegenerativas, Universidad de Valencia, Burjassot, Spain. [2]Present address: Sloan-Kettering Institute, Department of Developmental Biology, New York, New York, USA. Correspondence should be addressed to I.F. (isabel.farinas@uv.es).

Received 20 July; accepted 17 September; published online 8 November 2009; doi:10.1038/nn.2437

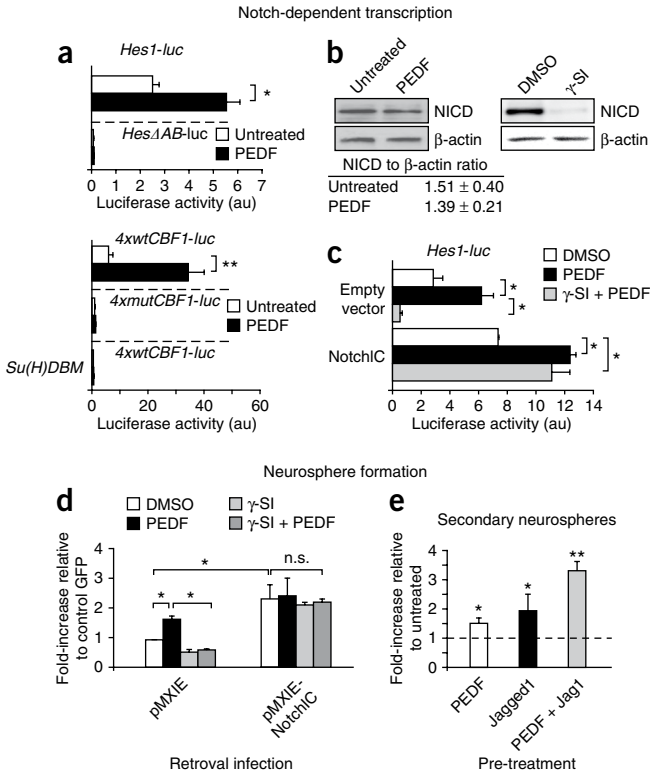

Figure 1 PEDF interaction with Notch signaling regulates Notch-dependent transcription and neurosphere formation. (**a**) Top, *Hes1* promoter activity in the absence or presence of PEDF for 24 h in cells transiently expressing luciferase reporter constructs that either contained (*Hes1-luc*) or lacked (*HesΔAB*-luc) CBF1-binding sites ($n = 4$). Bottom, activity of a specific artificial CBF1-dependent reporter that either contained consensus CBF1 recognition sequences (*4xwtCBF1-luc*) or a mutated form (*4xmutCBF1-luc*) in the absence or presence of PEDF for 24 h ($n = 3$). The effects of PEDF on CBF1-mediated transcription after genetic knockdown of Notch signaling by overexpression of a dominant negative form of CBF1 (*Su(H)DBM*) are shown. (**b**) NICD detection assessed by immunoblotting in untreated or PEDF-treated neurospheres (left) or after treatment with the γ-secretase inhibitor (γ-SI) L-658,458 (right). The table shows a quantification of the blots relative to endogenous β-actin levels ($n = 3$). Full-length blots are presented in **Supplementary Figures 7** and **11**. (**c**) The effects of PEDF on *Hes1* promoter activation after treatment with γ-SI in cells nucleofected with an empty vector or with a constitutively active NotchIC fragment ($n = 4$) are shown. (**d**) Number of neurospheres generated from cells that were infected with pMXIE or pMXIE-NotchIC–carrying retroviruses in the presence of PEDF, γ-SI or both ($n = 4$). (**e**) Fold-change in the number of secondary neurospheres formed by cultures treated with 20 ng ml^{-1} PEDF, 2 μg ml^{-1} Jagged1 (Jag1) or both (PEDF + Jag1), relative to those formed in the untreated condition ($n = 4$). Data are expressed as mean ± s.e.m. * $P < 0.05$ and ** $P < 0.01$.

of astroglia/radial glia-like NSCs and that the level of Notch activity correlated with neurosphere formation potential and multipotency. Moreover, we found that different levels of Notch activation could be inherited by the two daughter cells of a neurosphere-forming cell during its first mitotic division and that PEDF intensified Notch-dependent transcription in cells with low levels of Notch activation. Our biochemical data indicate that PEDF induced a non-canonical activation of the NFκB pathway leading to the dismissal of nuclear receptor co-repressor (N-CoR) from CBF1 sites in specific promoters, resulting in cells that were more undifferentiated and prone to mitogenic stimulation.

RESULTS

PEDF enhances Notch activity in adult NSCs

Because our previous observations indicate that PEDF increases NSC self-renewal and upregulates Hes1 and Hes5 expressions[9], we investigated possible interactions with Notch. PEDF activated a *Hes1-luciferase* reporter, but not a reporter lacking CBF1 sites (*HesΔAB-luc*)[22], in neurosphere-forming cells; similar results were obtained with CBF1 reporters (**Fig. 1a**). Expression of a dominant-negative form of CBF1 (*Su(H)DBM*) or pharmacological inhibition of the γ-secretase activity (**Fig. 1b**) essentially abolished the effects of PEDF on *Cbf1-* (also known as *Rbpj*) and *Hes1-luc* reporters, respectively, but γ-secretase inhibition could not block the effects of PEDF on Hes1 transcription in cells expressing a constitutively active Notch intracellular fragment (NotchIC[17]) (**Fig. 1a**,**c**), suggesting that PEDF's effects require an active Notch. The effects of PEDF on neurosphere formation were also dependent on Notch signaling, as overexpression of *Su(H)DBM* (**Supplementary Fig. 1**) or γ-secretase inhibition (**Fig. 1d**) prevented PEDF from increasing neurosphere numbers. However, PEDF did not promote Notch cleavage. NICD has been detected in neurospheres in the absence of added Notch ligands[23] and PEDF did not increase its level (**Fig. 1b**). Our results indicate that PEDF is not a Notch ligand, but can enhance Notch's transcriptional effects.

To test whether PEDF and Notch cooperated to regulate self-renewal, we seeded single cells in the presence of the Notch ligand Jagged1 and/or PEDF, dissociated the neurospheres after 4 d and plated the isolated cells in mitogens alone. Pre-stimulation with Jagged1 or PEDF alone increased self-renewing divisions, as the number of secondary neurospheres formed was higher than in the untreated condition. However, a more robust increase was obtained when the cells were treated with a combination of both molecules (**Fig. 1e**). Therefore, PEDF increased neurosphere formation and Hes1 transcription in concert with Notch, but appeared to be incapable of improving neurosphere formation when Notch signaling was very high (**Fig. 1d**).

We next analyzed Notch activity in the SEZ of TNR mice in which enhanced green fluorescent protein (EGFP) expression is under the control of four CBF1-responsive elements[2,19,20]. Immunohistochemistry revealed that 15–20% cells had detectable levels of NICD and different levels of EGFP intensity (EGFP^{hi} and EGFP^{lo} cells; **Fig. 2a**). A few EGFP-positive cells were ependymocytes, identified by position, morphology and S100β immunostaining; all of them had high CBF1 activity (**Fig. 2b**). However, 95% of the EGFP-positive cells were subependymal; virtually all these were positive for the astrocyte-specific L-glutamate/L-aspartate transporter (GLAST)[24], but not for the astrocyte terminal differentiation marker S100β, and the vast majority were also Sox2 and Ki67 positive (**Fig. 2b**,**c**). Consistently, subependymal EGFP-positive cells were rarely Mash1 or doublecortin positive (**Fig. 2c** and **Supplementary Fig. 2**). Not all of the GLAST and Sox2 double-positive cells exhibited CBF1 activity, as 22.2 ± 5.8% were EGFP^{hi}, 66.9 ± 6.0% were EGFP^{lo} and 39.2 ± 5.9% were EGFP negative. In contrast, all of the BrdU label-retaining cells (BrdU-LRCs) were EGFP positive (**Fig. 2d**). These data indicate that Notch activity is highly restricted to GLAST, Sox2 and Ki67 triple-positive BrdU-LRCs and adult NSCs exhibit different levels of Notch activity.

To test whether PEDF could activate Notch-dependent transcription *in vivo*, we infused PEDF for 24 h into the lateral ventricle of TNR mice injected with BrdU 3 weeks prior. The proportion of EGFP-positive, GLAST-negative cells did not increase after the infusion (4.0 ± 0.9% in PEDF versus 5.4 ± 0.5% in saline infusions, $n = 3$).

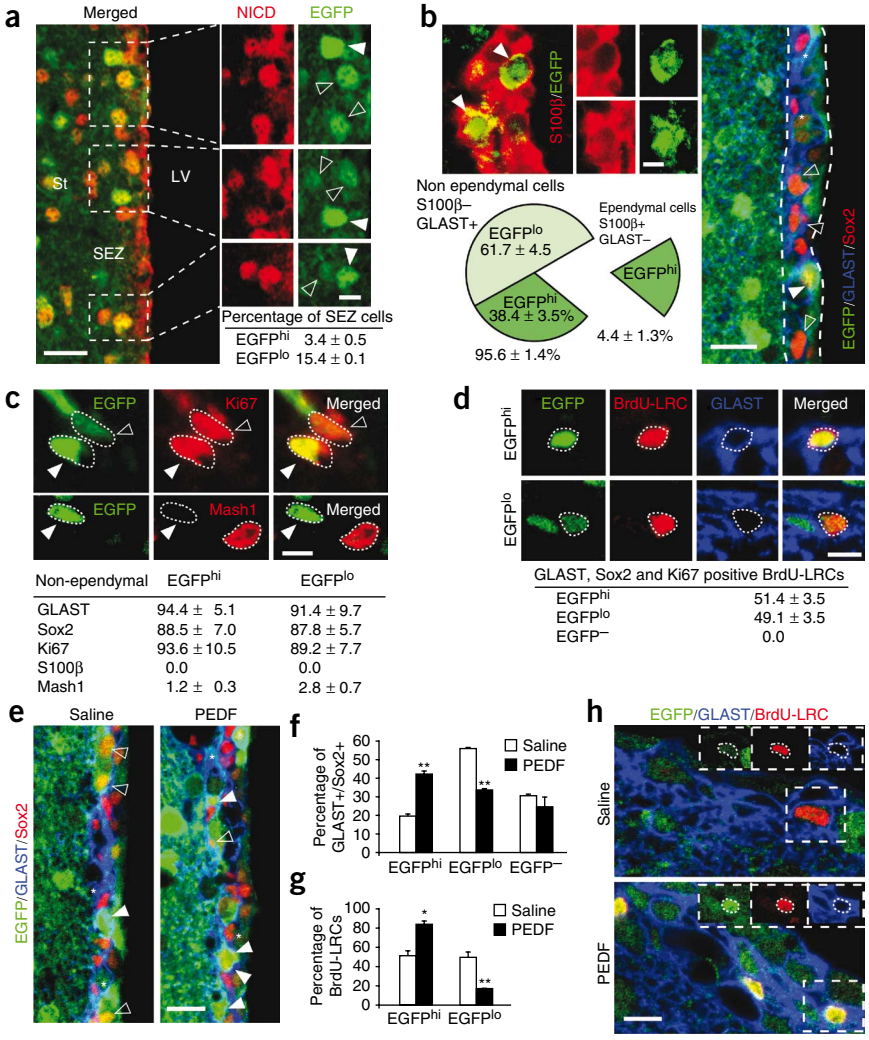

Figure 2 Notch signaling is restricted to GLAST and Sox2 double-positive cells and can be increased by PEDF infusion. (**a**) Immunofluorescence for EGFP and NICD in the SEZ of TNR mice with EGFP^{hi} and EGFP^{lo} cells, with both types containing NICD. The percentage of each cell type is shown in the table ($n = 5$). LV, lateral ventricle; St, striatum. (**b**) EGFP immunostaining revealed that there was high CBF-1 activity in S100β-positive ependymal cells. Right, immunofluorescence for GLAST, Sox2, and EGFP in TNR mice. Pie chart represents the distribution of ependymal and non-ependymal cells that were EGFP positive ($n = 5$). (**c**) EGFP^{hi} and EGFP^{lo} cells were Ki67 positive, but not Mash1 positive. The table contains the quantification for different markers in the subependymal EGFP^{hi} and EGFP^{lo} cell populations (percentage of cells that were marker positive, $n = 5$). Non-ependymal EGFP-positive cells in the SEZ of TNR mice were GLAST, Sox2 and Ki67 positive. (**d**) All of the cells retaining BrdU that was injected 3 weeks before the mice were killed (BrdU-LRCs) had CBF-1 activity (EGFP positive). The percentage of each EGFP-positive type is reflected in the table ($n = 5$). (**e**–**g**) PEDF infusion for 24 h increased the percentage of GLAST and Sox2 double-positive cells (**e**,**f**) or GLAST-positive BrdU-LRCs (**g**,**h**) with high CBF-1 activity at the expense of those with low CBF1 activation in TNR mice. In all cases, white arrowheads indicate EGF^{hi} cells, empty arrowheads indicate EGFP^{lo} cells and asterisks indicate EGF-negative cells. Data are expressed as mean ± s.e.m. * $P < 0.05$ and ** $P < 0.01$. Scale bars represent 20 μm (**a**,**b**,**e**) and 10 μm (**c**,**d**,**g**).

However, we found more GLAST and Sox2 double-positive cells with high levels of EGFP, at the expense of EGFP^{lo}, but not EGFP-negative cells, in PEDF- versus saline-infused mice (**Fig. 2e**,**f**). We also detected more EGFP^{hi} cells and fewer EGFP^{lo} BrdU-LRCs (**Fig. 2g**,**h**). These results are consistent with our molecular data showing that PEDF enhanced low levels of Notch transcriptional activity.

PEDF and Notch together promote stemness and multipotency

To investigate the neurosphere-forming potential of EGFP-positive cells, we seeded EGFP^{hi} and EGFP^{lo} fluorescence-activated cell sorting (FACS)-sorted cells at low density (**Fig. 3a–c**). More than 75% of the EGFP^{hi} cells, but only around 20% of the EGFP^{lo} cells, formed a neurosphere after 4 d (**Fig. 3b**,**c**). These differences were not a result of distinct survival (**Supplementary Fig. 3**), but of differential mitogenic activation; over 85% of the EGFP^{hi} cells had initiated a neurosphere, whereas more than 50% of the EGFP^{lo} cells remained single and viable 48 h after plating (**Supplementary Fig. 3**). EGFP-negative cells survived poorly, did not divide during the 48-h period and formed almost no neurospheres (**Supplementary Fig. 3**). Therefore, CBF1 activity correlates with NSC activation.

EGFP^{hi} cells formed larger neurospheres and maintained high subcloning efficiency, whereas EGFP^{lo} cells formed smaller neurospheres and their capacity to self-renew was lower and rapidly decreased in subsequent passages (**Fig. 3b**,**d** and **Supplementary Fig. 4**). To investigate whether the level of Notch activity also correlated with multipotency, we differentiated single neurospheres originating from EGFP^{hi} or EGFP^{lo} cells and scored clones containing different cell lineages after immunostaining for O4-positive oligodendrocytes, GFAP-positive astrocytes and βIII-tubulin–positive neurons (**Fig. 3e**). We analyzed multipotent versus astrocyte-only clones and found that EGFP^{hi} cells were substantially more multipotent than EGFP^{lo} cells (**Fig. 3f**). We obtained the same results when cells were seeded clonally (**Supplementary Fig. 5** and **Supplementary Fig. 6**). Thus, the level of Notch activation positively correlates with neurosphere potential, duration of self-renewal and multipotency.

To further analyze the interactions between Notch activity and PEDF, we cultured EGFP^{hi} and EGFP^{lo} cells with PEDF (primary) and subcultured them for two passages in the absence of PEDF (secondary and tertiary passages). PEDF increased mitogenic activation of EGFP^{lo} cells without altering their survival (**Supplementary Fig. 3**), resulting in higher numbers of spheres in low-density and clonal cultures (**Fig. 3c** and **Supplementary Fig. 6**). Furthermore, PEDF-treated EGFP^{lo} cell–derived neurospheres generated higher numbers of secondary and tertiary neurospheres on withdrawal of PEDF (**Fig. 3d**). Likewise, treatment with PEDF increased the frequency of tripotent EGFP^{lo} cell–derived neurospheres at the expense of astrocyte-only clones (**Fig. 3e**,**f** and **Supplementary Fig. 6**). These results indicate that PEDF can increase self-renewal potential and plasticity in cells with low levels of CBF1 activity.

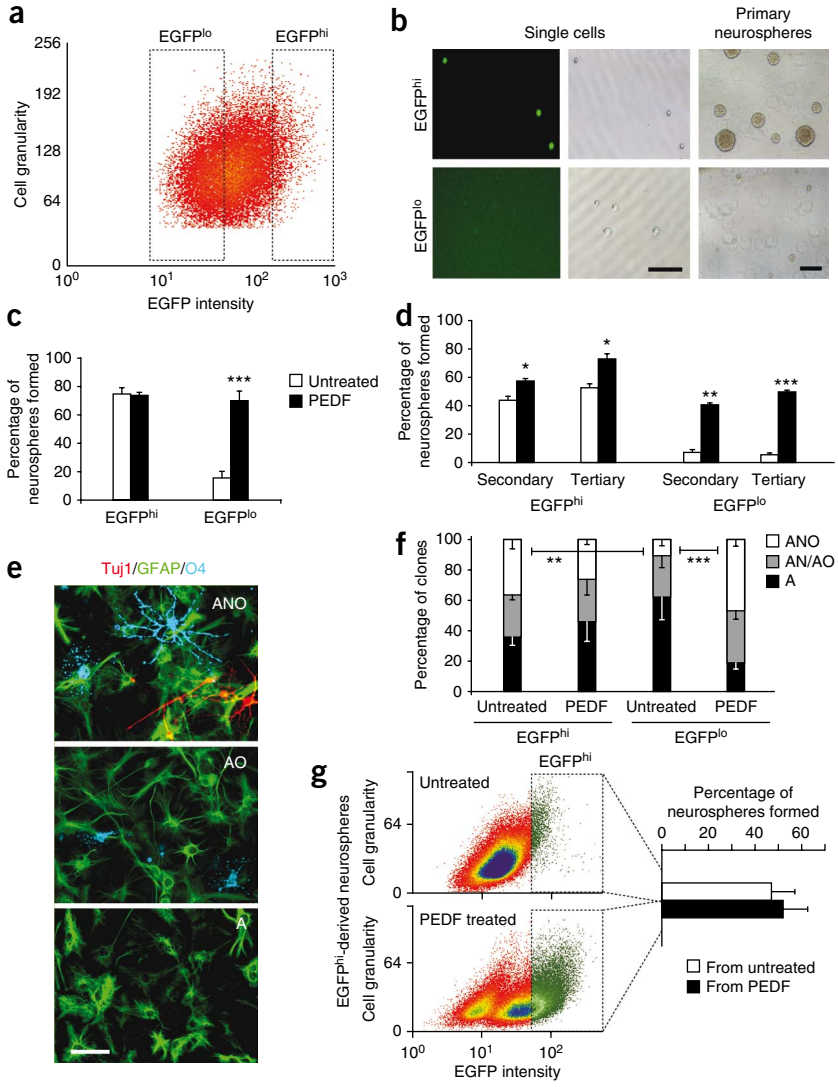

Figure 3 PEDF regulates self-renewal in concert with Notch transcriptional activity. (**a**) Representative FACS plot showing collection gates for viable EGFP^{hi} and EGFP^{lo} cells from TNR mice neurospheres. (**b**) Images of EGFP^{hi} and EGFP^{lo} sorted cells (fluorescence and phase contrast) and of derived neurospheres. (**c**) Quantification of the clonogenic capacity (as percentage of neurospheres formed relative to seeded cells at limiting dilution) of FACS-sorted EGFP^{hi} and EGFP^{lo} cells in the presence or absence of PEDF ($n = 8$). (**d**) Quantification of secondary and tertiary neurospheres in the absence of PEDF produced by cells from PEDF-grown primary neurospheres. (**e**) Representative images showing immunofluorescence for astrocytes (A, GFAP positive), neurons (N, neuronal βIII-tubulin positive) and oligodendrocytes (O, O4 positive) in isolated neurospheres differentiated for 7 d. (**f**) Distribution of unipotent (A), bipotent (A/N or A/O) and tripotent (ANO) clones among neurospheres derived from EGFP^{hi} and EGFP^{lo} cells (grown in the presence or in the absence of PEDF) differentiated for 7 d ($n = 3$ experiments from independent mice, at least 50 clones analyzed in each case). (**g**) PEDF treatment increased the number of self-renewing cells. FACS-sorted EGFP^{hi} cells treated with PEDF generated neurospheres that contained more EGFP^{hi} cells (FACS plots on the left) with high self-renewal capacity (right) ($n = 3$). Data are expressed as mean ± s.e.m. * $P < 0.05$, ** $P < 0.01$ and *** $P < 0.001$. Scale bars represent 100 μm (**b**) and 50 μm (**f**).

In contrast, PEDF increased neither the survival nor the potential of EGFP^{hi} cells to initially divide, produce primary spheres or differentiate to multiple lineages at either low or clonal cell density (**Fig. 3c–f** and **Supplementary Fig. 6**). PEDF-treated EGFP^{hi} cell–derived neurospheres did yield more secondary clones (**Fig. 3d**), suggesting that PEDF enhances Notch activity to maintain an immature phenotype and self-renewal potential in the daughters of EGFP^{hi} cells. Consistently, we observed that neurospheres formed by EGFP^{hi} cells in the presence of PEDF contained more cells with high CBF1-reporter activity and self-renewal than untreated neurospheres (**Fig. 3g**). These results suggest that PEDF maintains/induces CBF1 activity in dividing NSCs, leading to increased self-renewal and multi-differentiation potential.

PEDF and Notch modulate NSC division outcomes

Because PEDF increases self-renewing divisions in concert with Notch, we decided to study Notch activity during the first division of a NSC *in vitro* using a cell pair assay. Single cells were seeded for 24 h and immunostained with antibodies to NICD (specificity controls in **Supplementary Fig. 7**). In approximately 45% of the cell pairs, one daughter cell had high levels of NICD and the other had very low levels of NICD (NICD$^{hi/lo}$), whereas equivalent high levels of NICD were observed in the rest of the cell pairs (NICD$^{hi/hi}$) (**Fig. 4a,b**). Thus, Notch activity can be symmetrically or asymmetrically distributed. The proportion of NICD$^{hi/lo}$ and NICD$^{hi/hi}$ cell pairs did not change in the presence of PEDF (**Fig. 4b**), which is consistent with the observation that PEDF does not activate Notch upstream of CBF1.

The epidermal growth factor receptor (EGFR) can also be symmetrically or asymmetrically distributed in the progeny of dividing fetal neural progenitors[25]. In adult cultures, 50–55% of the cell pairs contained daughters with similar levels of the receptor (EGFR$^{hi/hi}$), whereas one daughter cell expressed high levels and the other one expressed very low levels of immunofluorescence (EGFR$^{hi/lo}$) in the remainder of the cell pairs (**Fig. 4c,d**). Notably, high NICD expression always correlated with high EGFR levels. This result, together with our observation that cells with high Notch activity are more prone to divide in EGF (**Supplementary Fig. 3**), suggests that Notch might regulate EGFR expression.

We therefore analyzed whether responses to EGF could be under the cooperative control of Notch and PEDF. Overexpression of NotchIC in our cells substantially activated transcription of an *Egfr-luc* reporter (containing the 5′ UTR and 980 bp of the proximal promoter; **Fig. 4e**), whereas overexpression of *Hes1* did not (relative luciferase activity ± s.e.m., 2.30 ± 0.52 in *Egfr-luc* and 2.82 ± 0.87 in *Egfr-luc* and *Hes1*-transduced cells, $n = 3$). Despite previous evidence that NICD does not activate the *Egfr-luc* reporter in a fibroblast cell line[26], *in silico* analysis identified two putative CBF1-binding sites in the *Egfr* proximal promoter (**Fig. 4f**). We therefore performed chromatin immunoprecipitation (ChIP) experiments to examine the physical interaction between NICD and CBF1 proteins and the putative CBF1-containing

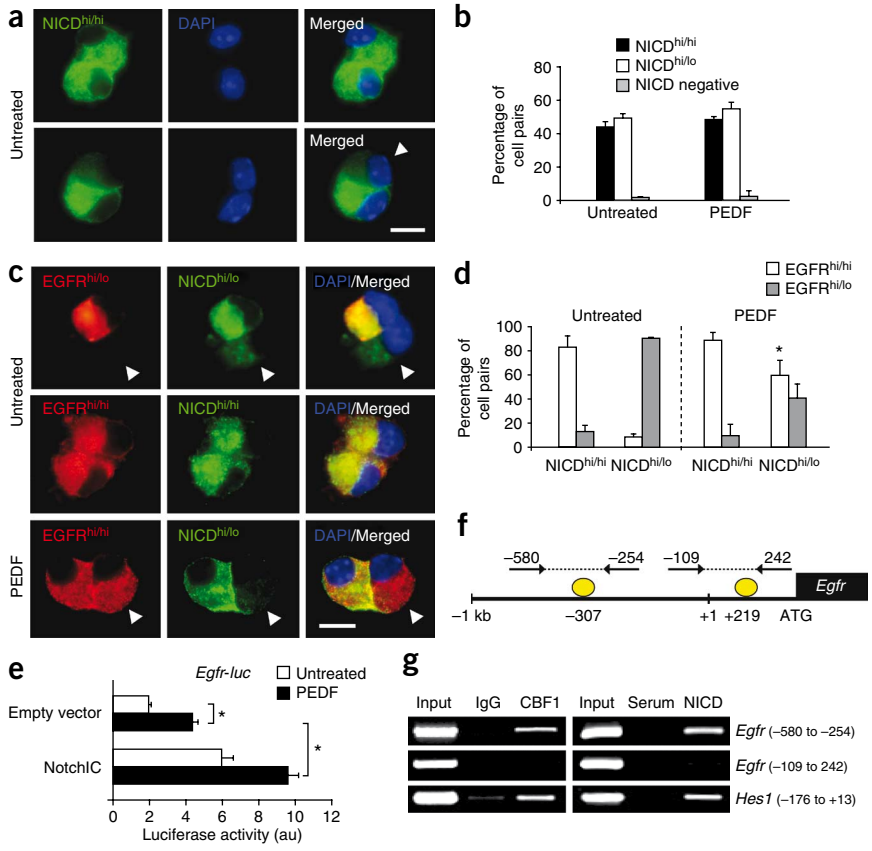

Figure 4 PEDF and Notch regulate EGF-dependent mitogenic response in adult NSCs. (**a**) Representative cell pairs resulting from a divided NSC immunostained for endogenous NICD showing NICD$^{hi/hi}$ (symmetrical) and NICD$^{hi/lo}$ (asymmetrical) distributions. Arrowhead indicates low levels of NICD. (**b**) PEDF treatment did not modify NICD distribution in cell pairs ($n = 4$, no less than 50 cell pairs each). (**c**) Immunofluorescence for EGFR and NICD in cell pairs showing symmetrical (hi/hi) or asymmetrical (hi/lo) distributions. (**d**) PEDF increased the number of EGFR$^{hi/hi}$ cell pairs at the expense of EGFR$^{hi/lo}$ pairs ($n = 4$). In untreated cultures, high NICD expression correlated with high EGFR expression. In PEDF-treated cultures, daughter cells with low NICD levels could have high levels of EGFR. (**e**) Luciferase assays for *Egfr* promoter activity in NotchIC-overexpressing cells with and without PEDF ($n = 4$). (**f**) Scheme depicting two putative sites (GTG GGA G at position –307 and GTG GGA C at position +219) that are homologous to the consensus CBF1 sequence (GTG GGA A) found by *in silico* analysis in the proximal promoter (–1 kb) and the 5′ UTR of the mouse *Egfr* gene. Arrows represent positions of primers used for ChIP analysis. (**g**) Representative PCR from ChIP analyses with antibodies to NICD and CBF1 and nonrelevant rabbit IgGs or control antiserum in the *Egfr* promoter. *Hes1* was used as a positive control (binding site between nucleotides –176 and +13) ($n = 4$). Full-length gels are presented in **Supplementary Figure 11**. Data are expressed as mean ± s.e.m. * $P < 0.05$. Scale bars represent 5 μm.

regions on the *Egfr* proximal promoter, using the *Hes1* promoter as a positive control[22]. Although antibodies to NICD and CBF1 failed to bind position +219, both were able to immunoprecipitate the *Egfr* promoter fragment containing the CBF1 site on position –307 (**Fig. 4g**). Consistent with a direct regulation of EGFR transcription by CBF1, we observed increased proportions of cells with undetectable expression of EGFR in *Su(H)DBM*-overexpressing cultures and increased EGFR symmetric distribution in the incipient daughters of dividing NotchIC-overexpressing NSCs (**Supplementary Fig. 8**).

As in the case of *Hes1* transcription, treatment with PEDF alone or in combination with NotchIC-overexpression promoted the activation of the *Egfr-luc* reporter and increased the proportion of NICD$^{hi/lo}$ cell pairs in which the cell with very low levels of NICD had detectable levels of EGFR (**Fig. 4c–e**). These data indicate that EGFR is a target of Notch and that PEDF can upregulate the expression of Notch-dependent stemness genes (for undifferentiation and mitogenic activation) when Notch levels are not maximal.

PEDF induces a gene-specific dismissal of repressor N-CoR

Notch activity relies on a complex interplay between transcriptional coactivators and co-repressors that ultimately sets the threshold of the response[14]. N-CoR was initially identified as a co-repressor for unliganded hormone nuclear receptors, but it can partner with a variety of transcription factors including CBF1 (refs. 27–29). Analyses in mutant mice have revealed a requirement for N-CoR in the inhibition of Notch-induced astrogliogenesis in the developing brain[27], but N-CoR function and regulation in adult NSCs is largely unknown. N-CoR was present in the nuclei of most dissociated neurosphere cells, but 18.2 ± 5.2% of the cells had detectable levels of cytoplasmic N-CoR and this percentage rose in PEDF-treated cultures (36.0 ± 3.6%, $n = 4$, $P < 0.01$; **Fig. 5a**). Immunoblot detection in cellular fractionates also revealed that PEDF treatment increased the cytoplasmic levels of N-CoR (**Fig. 5b**). Therefore, N-CoR moves from a nuclear to a cytoplasmic location in response to PEDF.

Given that PEDF enhances Notch induction of *Hes1* and *Egfr* expression, we next examined whether CBF1-binding sites in the promoters of these genes were occupied by N-CoR and whether PEDF induced the dismissal of N-CoR from these sites. In nonstimulated cells, antibodies to N-CoR immunoprecipitated genomic DNA fragments containing known CBF1-binding sites in the *Hes1* promoter[22] and the putative binding site at position –307 in the *Egfr* promoter, but not the site at +219 or control distal regions on both promoters. (**Fig. 4f** and **Supplementary Fig. 9**), suggesting that N-CoR directly represses transcription of these genes. In PEDF-treated cultures, there was a decrease in the association of N-CoR with both promoters (**Fig. 5c**). The *Gfap* proximal promoter contains one putative repressor domain harboring a conserved CBF1 consensus-binding site that can bind CBF1 and N-CoR, and CNTF-induced dismissal of N-CoR from this site promotes astrocytic differentiation of fetal progenitors[27]. In nonstimulated adult NSCs, N-CoR also bound the *Gfap* promoter, but PEDF did not cause its displacement (**Fig. 5c**). Consistently, PEDF treatment did not increase the levels of *Gfap* mRNA (*Gfap* to *Actb* ratio ± s.e.m.: control, 3.2 ± 0.8; PEDF, 2.9 ± 0.5; $n = 3$). ChIP analysis on the promoter of the immune-specific *Ptcra* gene[30] revealed that N-CoR binding to CBF1 sites was not modified by PEDF treatment (**Supplementary Fig. 9**). These data indicate that PEDF has a role in the modulation of Notch dependent genes that differs from that of other N-CoR regulators.

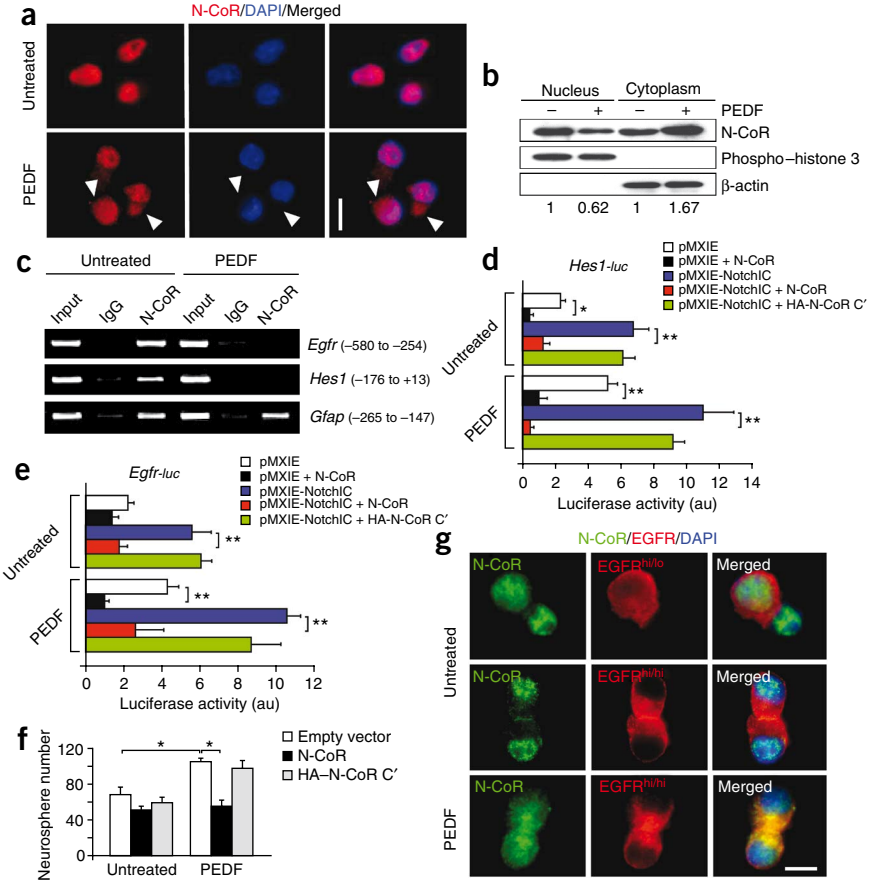

Figure 5 PEDF regulates Notch-dependent transcription and self-renewal by inducing the dismissal of N-CoR. (**a**) N-CoR immunoreactivity and nuclear DAPI staining in untreated cells or after 24 h of PEDF treatment. Arrowheads indicate cytoplasmic N-CoR labeling ($n = 4$). (**b**) Western blot from nuclear and cytoplasmic extracts of cells treated with PEDF for 24 h. PEDF treatment increased the amount of N-CoR in the cytoplasm at expense of nuclear N-CoR. Numbers indicate the ratio between the treated and untreated conditions. Specificity controls for N-CoR and phospho-histone H3 antibodies are presented in full-length immunoblots in **Supplementary Figure 11**. (**c**) ChIP assays in untreated and PEDF-treated cells using nonrelevant rabbit IgGs or antibodies to N-CoR and primers flanking the CBF1-binding sites in *Egfr*, *Hes1* and *Gfap* promoters ($n = 4$). Uncropped gel images are presented in **Supplementary Figure 11**. (**d**,**e**) Overexpression of wild-type N-CoR, but not of its repression-dead form (*HA–Ncor1-C′*), completely abolished PEDF-induced Hes1 and EGFR transactivation in the presence of endogenous levels of NICD and in NotchIC-overexpressing cells ($n = 4$). (**f**) Overexpression of N-CoR, but not of its CBF1-binding mutant form, abrogated the effects of PEDF on self-renewal ($n = 4$). (**g**) Colocalization of endogenous N-CoR and EGFR in cell pairs formed in the absence or presence of PEDF for 24 h. Symmetric distribution of EGFR after PEDF treatment largely correlated with N-CoR cytoplasmic distribution ($n = 4$). Data are expressed as mean ± s.e.m. * $P < 0.05$ and ** $P < 0.01$. Scale bars represent 10 μm (**a**) and 5 μm (**g**).

Consistent with an N-CoR–dependent regulation of Hes1 and EGFR transcription, overexpression of full-length *Ncor1*, but not of its repression-dead form (a truncated *HA–Ncor1-C′* lacking CBF1 sites)[27], completely blocked the positive effects elicited by NotchIC overexpression or PEDF treatment on *Hes1* and *Egfr* reporters (**Fig. 5d**,**e**). Overexpression of *Ncor1*, but not *HA–Ncor1 C′*, also blocked the increased clonogenic capacity induced by NotchIC (**Supplementary Fig. 9**) or PEDF (**Fig. 5f**). These results indicate that PEDF-induced N-CoR redistribution enhances Notch transcriptional activity at the *Hes1* and *Egfr* genes, leading to self-renewal. Consistent with this model, 78.3 ± 3.3% of the EGFR$^{hi/hi}$ cell pairs in untreated cultures, but only 39.5 ± 9.6% of the EGFR$^{hi/hi}$ cell pairs in PEDF-treated cultures, expressed nuclear N-CoR (**Fig. 5g**).

PEDF-induced dismissal of N-CoR is NF-κB/p65 dependent

Although little is known about the intracellular pathways activated by PEDF, its pro-survival effects are mediated by NF-κB[31,32]. Because the NF-κB subunit p65 is expressed by GFAP-positive SEZ cells[33], we investigated whether this pathway was involved in signaling PEDF effects on NSCs. In nonstimulated cells, silent NF-κB complexes reside in the cytoplasm in combination with inhibitory proteins of the IκB family, but, following degradation of IκB proteins induced by stimulus-coupled phosphorylation, p65 translocates to the nucleus, where it activates transcription[34]. We were able to abolish the PEDF-induced activation of *Hes1* and *Egfr* promoters in NotchIC-transduced NSCs with the addition of the NF-κB pharmacological inhibitor BAY11-7082 (**Fig. 6a**). PEDF's effects on neurosphere formation were also abrogated in the presence of BAY11-7082 (data not shown) and in cells overexpressing the constitutive repressor of NF-κB, SR-IκB$_{(32–36)}$[35] (**Fig. 6b**). Therefore, activation of NF-κB is required for PEDF's effects in Notch-competent NSCs.

More specifically, the actions of PEDF on neurosphere formation were abrogated in cells transduced with a p65–NF-κB mutant that lacked the nuclear export signal and the transactivation domain (*p65ΔNES*)[36]. Ectopic expression of a p65–NF-κB mutant that only lacked the transactivation domain (*p65ΔTA*)[36], however, did not block the increase in neurosphere number (**Fig. 6b**). Consistent with the suggestion that PEDF actions require p65 nuclear export, PEDF's effects on neurosphere formation were blocked with the addition of the pharmacological inhibitor of nuclear export leptomycin B (LMB; fold-increase in neurosphere number relative to EGF + fibroblast growth factor 2 ± s.e.m.: PEDF, 1.48 ± 0.03; PEDF+LMB, 0.95 ± 0.03; $n = 3$, $P < 0.01$). Thus, PEDF's actions on self-renewal require nucleo-cytoplasmic shuttling of p65, but not p65-dependent transcription of NFκB-target genes.

Using simultaneous immunofluorescent detection of endogenous p65 and N-CoR in PEDF-treated NSCs, we found a temporal correlation in their redistribution to the cytoplasm (**Fig. 6c**). Moreover, overexpression of *p65ΔNES* resulted in a persistent N-CoR nuclear signal even in the presence of PEDF (**Fig. 6d**), suggesting that p65 export is functionally required for PEDF-induced N-CoR redistribution. Immunoprecipitation experiments with antibodies to N-CoR followed by immunoblot for p65 in cytoplasmic and nuclear fractions revealed a physical interaction between p65 and N-CoR in both subcellular fractions in control conditions; treatment with PEDF, however, decreased the amount of p65 that could be recovered from the nucleus by N-CoR immunoprecipitation and increased the levels of cytoplasmic N-CoR/p65 complexes (**Fig. 6e**). Thus, p65 forms a

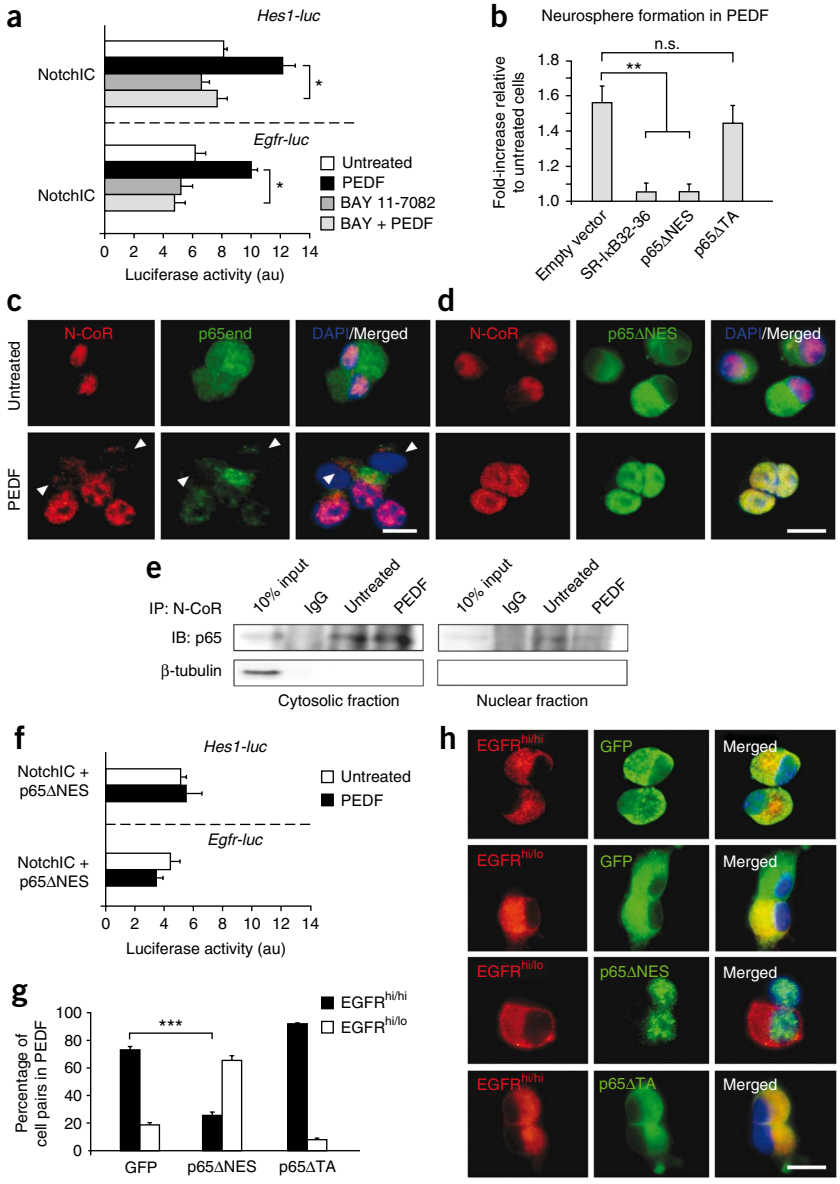

Figure 6 PEDF promotes dismissal of N-CoR by inducing NFκB-p65. (**a**) Application of 0.5 μM BAY11-7082 blocked the effects of PEDF on *Egfr*- and *Hes1-luciferase* reporter activities in NotchIC-expressing cells ($n = 3$). (**b**) Overexpression of SR-I$\kappa B_{32–36}$ and p65ΔNES, but not p65ΔTA, abolished PEDF-induced increases in neurosphere formation ($n = 5$). (**c**) Immunofluorescence for endogenous p65 and N-CoR in untreated and PEDF-treated cells 24 h after plating. Arrowheads indicate p65 and N-CoR cytoplasmic colocalization ($n = 3$). (**d**) Immunofluorescence with p65 and N-CoR antibodies to detect transiently expressed p65ΔNES and endogenous N-CoR. Overexpression of p65ΔNES blocked N-CoR nuclear export ($n = 4$). (**e**) Immunoprecipitation (IP) of N-CoR from cytosolic and nuclear fractions of untreated or PEDF-treated cells, performed with nonrelevant rabbit IgG or with antibodies to N-CoR, followed by immnunoblotting (IB) with p65 antibodies ($n = 3$). Full-length blots are presented in **Supplementary Figure 11**. (**f**) p65ΔNES overexpression abrogated *Egfr* and *Hes1* promoter activity in NotchIC-overexpressing cells treated with PEDF ($n = 4$). (**g**) Quantification of $EGFR^{hi/hi}$ and $EGFR^{hi/lo}$ cell-pair distributions in cultures of GFP-, p65ΔTA- and p65ΔNES-transduced cells after PEDF treatment for 24 h ($n = 5$, no less than 50 cell pairs were scored for each condition). (**h**) Representative cell pairs as immunostained for EGFR and NICD in PEDF-treated cells that were previously transduced with GFP or p65ΔNES. Data are expressed as mean ± s.e.m. * $P < 0.05$, ** $P < 0.01$ and *** $P < 0.001$. n.s., not significant, $P \geq 0.05$. Scale bars represent 10 μm.

complex with N-CoR that moves from the nucleus to the cytoplasm and this shuttling becomes enhanced in response to PEDF.

Consistent with the possibility that PEDF enhances Notch activity through NF-κB signaling and subcellular p65 redistribution, induction of *Hes1* and *Egfr* transcription by PEDF were abrogated in NSCs overexpressing *p65ΔNES* (**Fig. 6f**). Moreover, overexpression of *p65ΔNES*, but not *p65ΔTA*, reduced the proportion of PEDF-induced $EGFR^{hi/hi}$ cell pairs at the expense of $EGFR^{hi/lo}$ cell pairs (**Fig. 6g,h**). NSC division in PEDF therefore results in two daughter cells that have high levels of EGFR, both of which are capable of neurosphere formation, and this effect is dependent on p65-mediated N-CoR nuclear export.

Endogenous PEDF regulates N-CoR *in vivo*

Immunocytochemistry in the SEZ revealed cells with detectable levels of nuclear or cytoplasmic N-CoR (**Fig. 7a**). In TNR mice infused with PEDF for 24 h, overall CBF1-reporter levels were increased and N-CoR distribution appeared to be more cytoplasmic than in saline-infused mice (**Fig. 7b**). PEDF induced a 60% reduction in EGFP-positive BrdU-LRCs with nuclear N-CoR, concomitantly increasing cells with cytoplasmic N-CoR (**Fig. 7c,d**). Consistent with our molecular data showing that Notch- and PEDF-induced redistribution of N-CoR regulate the expression of EGFR, 92.3 ± 3.1% of GLAST and Sox2 double-positive BrdU-LRCs that were $EGFP^{hi}$ in PEDF-infused mice had high levels of this receptor. This resulted in higher proportions of EGFP and EGFR double-positive cells among GLAST and Sox2 double-positive cells after PEDF infusion; notably, we could observe cell pairs of $EGFP^{hi}$, GLAST-positive cells with high levels of EGFR *in vivo*, which was suggestive of potential NSC symmetrical divisions (**Fig. 7e–g**).

In a previous study, we infused PEDF or a C-terminal fragment capable of antagonizing PEDF effects for 7 d into the lateral ventricle of mice injected with BrdU 3 weeks previously. PEDF increased the number of BrdU-LRCs and primary neurosphere recovery, whereas the C-terminal PEDF fragment yielded BrdU-LRC numbers that were similar to those of saline-infused mice, but yielded fewer primary neurospheres[9]. Immunostaining with antibodies to N-CoR and BrdU in these mice revealed that the number of BrdU-LRCs with nuclear N-CoR was increased in PEDF-infused brains and decreased in C-terminal PEDF–infused brains compared with vehicle-infused ones (**Fig. 7h,i**). We also found increased proportions of BrdU-LRCs with high levels of EGFR in PEDF-infused than in saline- or C-terminal PEDF–infused brains (**Fig. 7j,k**). Virtually all of the BrdU-LRCs detected in the different infusion conditions were Ki67 positive (**Supplementary**

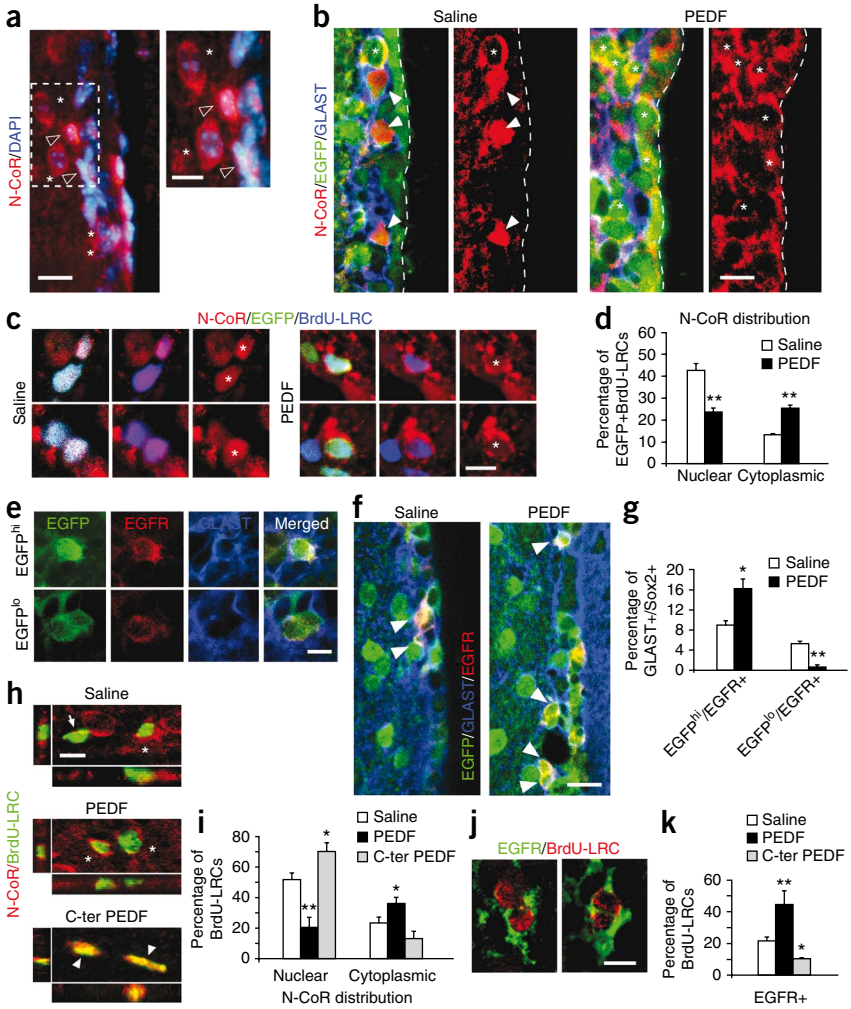

Figure 7 Endogenous PEDF regulates N-CoR subcellular distribution and activation of NSCs. (**a**) N-CoR in SEZ cells can be nuclear (arrowhead) or cytoplasmic (asterisk). Right, higher magnification of the region outlined by the dashed line. (**b**) Confocal immunofluorescence for N-CoR, EGFP and GLAST in infused TNR mice showing cytoplasmic (asterisk) or nuclear (arrowheads) distribution of N-CoR. (**c**) Immunofluorescence for N-CoR, EGFP and BrdU in infused TNR mice. (**d**) Quantification of EGFP-positive BrdU-LRCs in the SEZ of infused TNR mice ($n = 3$, over 50 BrdU-positives cells were analyzed per sample). (**e**) Coincidence of EGFP and EGFR levels in the GLAST-positive population. $EGFP^{hi}$ cells had higher levels of EGFR than $EGFP^{lo}$ cells. (**f**) Immunofluorescence for EGFP, EGFR and GLAST in infused TNR mice. Arrowheads indicate $EGFP^{hi}$, EGFR-positive cells. (**g**) PEDF infusion increased the percentage of $EGFP^{hi}$, GLAST-positive cells expressing EGFR. (**h**) Confocal images and *xz* (bottom) and *yz* (left) orthogonal projections of BrdU-LRCs (green) after saline, PEDF or C-terminal PEDF infusions, showing absence of N-CoR immunoreactivity (arrows) or staining for N-CoR (red) in the cytoplasmic (asterisks) or nuclear (arrowheads) compartments. (**i**) PEDF infusion decreased and C-terminal PEDF infusion increased the proportion of cells with nuclear N-CoR ($n = 3$). (**j**) Confocal images of BrdU and EGFR immunostaining. (**k**) PEDF, but not C-terminal PEDF, infusion increased the proportion of BrdU-LRCs expressing EGFR ($n = 3$). Data are expressed as mean ± s.e.m. * $P < 0.05$ and ** $P < 0.01$. Scale bars represent 20 µm (**a**,**b**,**f**) and 10 µm (**c**,**e**,**h**,**j** and inset in **a**).

Fig. 10), indicating that cycling label-retaining, but not terminally differentiated, cells were scored in our experiments. Thus, N-CoR subcellular redistribution induced by PEDF correlates with higher proportions of BrdU-LRCs with detectable levels of EGFR. These results indicate that endogenous PEDF acts physiologically to cause the dismissal of specific N-CoR repressor complexes, resulting in activation of Notch-regulated stem cell–related genes.

DISCUSSION

We found that the balance between symmetric and asymmetric divisions in NSCs can be modulated by endogenous PEDF's effects on Notch transcriptional activity. Mechanistically, PEDF promotes self-renewing divisions and maintenance of a multipotent state in NSCs by inducing the dismissal of transcriptional co-repressor N-CoR from its binding to CBF1 in specific promoters through a non-canonical activation of the NF-κB pathway. Because PEDF has a physiological role in the adult SEZ[9], we propose that PEDF is a natural modulator of N-CoR in endogenous niches contributing to stem-cell maintenance by interaction with the Notch pathway.

Notch is active in radial glia-like cells of neurogenic regions and downregulation of this pathway is required for lineage progression[20,21]. Consistently, we found that CBF1 activity in subependymal cells was detected together with B cell marker combinations (some ependymal cells were also labeled, consistent with a recent report[37]), and Notch activity levels positively correlated with *in vitro* stem potential. Our results indicate that $EGFP^{lo}$ cells also have stem-cell attributes, but their potential *in vitro* was reduced, consistent with a lineage progression from $EGFP^{hi}$ cells to $EGFP^{lo}$ cells. The effects of PEDF on the modulation of Notch and self-renewal indicate that some cells with low Notch expression can respond to cues that will retard their differentiation. However, although treatment of $EGFP^{lo}$ cells with PEDF resulted in a more extended self-renewing capacity, the treatment could not induce a self-renewal as extensive as that seen in $EGFP^{hi}$ cells. Moreover, many $EGFP^{lo}$ cells became refractory (probably those with very low Notch expression); for example, if grown neurospheres are treated with PEDF, they do not produce more secondary neurospheres[9], suggesting that PEDF signaling needs to be coincident with downregulation of Notch signaling during cell division. This is consistent with the finding that once CBF1 signaling has become attenuated in fetal neural progenitors, forced activation of CBF1 is ineffective at reverting them to NSCs[20].

Despite indirect evidences indicating that PEDF can regulate γ-secretase/presenilin-1 activity in endothelial cells[38], our data support a model in which PEDF cooperates with Notch only at the transcriptional level. In the CNS, only the *Hes1*, *Hes5* and *Blbp* (encoding the brain lipid-binding protein, also known as *Fabp7*) genes have been experimentally linked to CBF1 activation[13]. We found that the *Egfr* promoter is a target of CBF1, providing a molecular basis for the effects of Notch activation on proliferation. Because NSCs with high levels of EGFR generate more neurospheres *in vitro* and activated GFAP-positive B cells in the SEZ express EGFR[39,40], our results suggest that Notch probably determines self-renewing potential, at least in

part, by modulating mitogenic responsiveness. On the other hand, the Notch pathway has a dominant function in inhibiting differentiation of NSCs, as Hes1/5 repress execution of neurogenic programs[13,41]. Recent evidence indicates that Hes1 prevents permanent cell-cycle exit, allowing for reversibility of the quiescent state[42]. Therefore, coordinated expression of EGFR and Hes1 may determine stemness by promoting mitogenic response in a highly regulated quiescent population and nondifferentiation in a concerted way.

It has been reported that adipose triglyceride lipase (desnutrin or $iPLA_2\zeta$) is a putative receptor for PEDF in retinal epithelial cells[11] and PEDF can indeed regulate triglyceride metabolism in hepatocytes through adipose triglyceride lipase[43]. However, the compound (R)-bromoenol lactone, which irreversibly blocks 90% of the enzyme lipase activity[43], was ineffective at blocking PEDF's effects on neurosphere formation (C.A.-A. and I.F., unpublished data). Although PEDF mediates its effects on NSCs through an unknown receptor, our data indicate that PEDF's actions require activation of the NF-κB pathway. The Notch and NF-κB pathways have been shown to interact in various ways[44,45]. In particular, p65 induces nucleo-cytoplasmic translocation of N-CoR and *Hes1* transcription in a cell line[45]. GFAP-positive cells in the SEZ express components of the Notch and NF-κB signaling pathways[33,46] and N-CoR, and we found that the actions of PEDF do not require p65-dependent transcription of target genes, but instead require p65 subcellular redistribution. Regulation of the NF-κB pathway is complex, involving not only post-translational modifications in NF-κB complexes or target gene histones, but also the continuous nucleo-cytoplasmic shuttling of NF-κB[34]. We found that N-CoR bound to p65, although our data do not exclude the possibility that other molecules, such as IκB, could be implicated in the physical re-distribution of N-CoR from the nucleus to the cytoplasm[44].

Maintenance of a stem-cell state depends on the combined action of different gene products and it may therefore involve the activity of large regulatory complexes, including transcriptional co-repressors/activators and chromatin remodeling factors[47]. Our results suggest that modulation of N-CoR in response to various signals operating in endogenous niches could orchestrate the coordinated expression of molecules involved in the regulation of stem-cell proliferation and multipotency. Other pathways in distinct cellular settings regulate N-CoR differently. Dismissal from the *Gfap* promoter is induced in fetal NSCs in response to CNTF and N-CoR deletion results in cortical progenitors with impaired self-renewal that spontaneously differentiate into astroglial-like cells[27]. Notably, Notch activation during NSC differentiation appears to be pro-gliogenic[41]. Thus, our results indicate that Notch's opposing actions on self-renewal and astrogliogenesis could be determined by selective modulation of N-CoR repressive activity. Many transcriptional modulators are regulated by post-translational modification and MEK kinase and Akt kinase-dependent phosphorylation are involved in mediating the nuclear export of N-CoR in response to CNTF[27,48]. Further studies will be needed to determine how N-CoR specificity is mechanistically regulated in response to PEDF or other factors.

Analysis in cell pair assays and in cell populations that differ in Notch activity levels indicate that Notch asymmetry/symmetry at stem-cell division is functionally important for the outcome of the replication process[2]. It is unclear how asymmetric distribution of activated Notch is produced in adult NSCs although it may depend on the regulated partitioning of effectors such as Numb, which inhibits Notch signaling and whose segregation is dictated by cell-polarity determinants[1]. Our data indicate that symmetry/asymmetry can also be modulated by extrinsic cues and microenvironments, and, more specifically, neurovascular niches can modify stem-cell fate decisions that probably determine their persistence and response to nonphysiological demand.

METHODS

Methods and any associated references are available in the online version of the paper at http://www.nature.com/natureneuroscience/.

Note: Supplementary information is available on the Nature Neuroscience website.

ACKNOWLEDGMENTS

We are grateful to A. Bigas, J.L. de la Pompa, N. Gaiano, W.C. Greene, O. Hermanson, S. Hitoshi, A. Israel, K. Jepsen, M. Karin, R. Kopan, G. Leclercq, M.G. Rosenfeld, S. Sun, D. van der Kooy, Y. Zhan and V. Meni for kindly providing constructs and reagents. We also thank E. Porlan and H. Mira for technical advice, M. P. Rubio for excellent technical assistance, and E. Porlan and S. R. Ferrón for critical reading of the manuscript and valuable discussions. We gratefully acknowledge the help of M.A. Marqués-Torrejón with the infusion experiments and of A. Martínez and D. Gil with cytometry. We are also grateful to E. Lai for comments on the manuscript. This work was supported by grants from Ministerio de Ciencia e Innovación (SAF Program), Ministerio de Sanidad (Red Tercel, Centro de Investigación Biomédica en Red sobre Enfermedades Neurodegenerativas, CIBERNED), Generalitat Valenciana (Programa Prometeo) and Fundación 'la Caixa'. C.A. was a recipient of a Formación del Profesorado Universitario predoctoral fellowship. J.M.M.-R. and A.C.D. were funded by CIBERNED.

AUTHOR CONTRIBUTIONS

All of the authors designed and discussed the experiments. C.A.-A. conducted most of the cell culture and biochemistry experiments on the relationship between PEDF and Notch, Notch/EGFR asymmetry and the role of N-CoR and p65, as well as the infusion experiments and *in vivo* analyses. C.A.-A. and J.M.M.-R. performed the FACS experiments and analyses with TNR cells, ChIP studies and luciferase assays. A.C.D. contributed to immunohistochemistry analyses and multipotency assays. I.F. supervised the project and wrote the manuscript.

COMPETING INTERESTS STATEMENT

The authors declare competing financial interests: details accompany the full-text HTML version of the paper at www.nature.com/natureneuroscience/.

Published online at http://www.nature.com/natureneuroscience/.
Reprints and permissions information is available online at http://www.nature.com/reprintsandpermissions/.

1. Morrison, S.J. & Kimble, J. Asymmetric and symmetric stem-cell divisions in development and cancer. *Nature* **441**, 1068–1074 (2006).
2. Wu, M. *et al.* Imaging hematopoietic precursor division in real time. *Cell Stem Cell* **1**, 541–554 (2007).
3. Riquelme, P.A., Drapeau, E. & Doetsch, F. Brain micro-ecologies: neural stem cell niches in the adult mammalian brain. *Phil. Trans. R. Soc. Lond. B* **363**, 123–137 (2008).
4. Zhao, C., Deng, W. & Gage, F.H. Mechanisms and functional implications of adult neurogenesis. *Cell* **132**, 645–660 (2008).
5. Palmer, T.D., Willhoite, A.R. & Gage, F.H. Vascular niche for adult hippocampal neurogenesis. *J. Comp. Neurol.* **425**, 479–494 (2000).
6. Shen, Q. *et al.* Adult SVZ stem cells lie in a vascular niche: a quantitative analysis of niche cell-cell interactions. *Cell Stem Cell* **3**, 289–300 (2008).
7. Tavazoie, M. *et al.* A specialized vascular niche for adult neural stem cells. *Cell Stem Cell* **3**, 279–288 (2008).
8. Shen, Q. *et al.* Endothelial cells stimulate self-renewal and expand neurogenesis of neural stem cells. *Science* **304**, 1338–1340 (2004).
9. Ramírez-Castillejo, C. *et al.* Pigment epithelium-derived factor is a niche signal for neural stem cell renewal. *Nat. Neurosci.* **9**, 331–339 (2006).
10. Tombran-Tink, J. & Barnstable, C.J. PEDF: a multifaceted neurotrophic factor. *Nat. Rev. Neurosci.* **4**, 628–636 (2003).
11. Notari, L. *et al.* Identification of a lipase-linked cell membrane receptor for pigment epithelium–derived factor. *J. Biol. Chem.* **281**, 38022–38037 (2006).
12. Chiba, S. Notch signaling in stem cell systems. *Stem Cells* **24**, 2437–2447 (2006).
13. Louvi, A. & Artavanis-Tsakonas, S. Notch signaling in vertebrate neural development. *Nat. Rev. Neurosci.* **7**, 93–102 (2006).
14. Bray, S.J. Notch signaling: a simple pathway becomes complex. *Nat. Rev. Mol. Cell Bio.* **7**, 678–689 (2006).
15. Alexson, T.O., Hitoshi, S., Coles, B.L., Bernstein, A. & van der Kooy, D. Notch signaling is required to maintain all neural stem cell populations—irrespective of spatial or temporal niche. *Dev. Neurosci.* **28**, 34–48 (2006).
16. Androutsellis-Theotokis, A. *et al.* Notch signalling regulates stem cell numbers *in vitro* and *in vivo*. *Nature* **442**, 823–826 (2006).

17. Hitoshi, S. *et al.* Notch pathway molecules are essential for the maintenance, but not the generation, of mammalian neural stem cells. *Genes Dev.* **16**, 846–858 (2002).
18. Ohtsuka, T., Sakamoto, M., Guillemot, F. & Kageyama, R. Roles of the basic helix-loop-helix genes *Hes1* and *Hes5* in expansion of neural stem cells of the developing brain. *J. Biol. Chem.* **276**, 30467–30474 (2001).
19. Duncan, A.W. *et al.* Integration of Notch and Wnt signaling in hematopoietic stem cell maintenance. *Nat. Immunol.* **6**, 314–322 (2005).
20. Mizutani, K., Yoon, K., Dang, L., Tokunaga, A. & Gaiano, N. Differential Notch signaling distinguishes neural stem cells from intermediate progenitors. *Nature* **449**, 351–355 (2007).
21. Breunig, J.J., Silbereis, J., Vaccarino, F.M., Sestan, N. & Rakic, P. Notch regulates cell fate and dendrite morphology of newborn neurons in the postnatal dentate gyrus. *Proc. Natl. Acad. Sci. USA* **104**, 20558–20563 (2007).
22. Jarriault, S. *et al.* Signaling downstream of activated mammalian Notch. *Nature* **377**, 355–358 (1995).
23. Campos, L.S., Decker, L., Taylor, V. & Skarnes, W. Notch, epidermal growth factor receptor, and beta1-integrin pathways are coordinated in neural stem cells. *J. Biol. Chem.* **281**, 5300–5309 (2006).
24. Mori, T. *et al.* Inducible gene deletion in astroglia and radial glia—a valuable tool for functional and lineage analysis. *Glia* **54**, 21–34 (2006).
25. Sun, Y., Goderie, S.K. & Temple, S. Asymmetric distribution of EGFR receptor during mitosis generates diverse CNS progenitor cells. *Neuron* **45**, 873–886 (2005).
26. Zhang, Y.W. *et al.* Presenilin/gamma-secretase–dependent processing of beta-amyloid precursor protein regulates EGF receptor expression. *Proc. Natl. Acad. Sci. USA* **104**, 10613–10618 (2007).
27. Hermanson, O., Jepsen, K. & Rosenfeld, M.G. N-CoR controls differentiation of neural stem cells into astrocytes. *Nature* **419**, 934–939 (2002).
28. Kao, H.Y. *et al*. A histone deacetylase co-repressor complex regulates the Notch signal transduction pathway. *Genes Dev.* **12**, 2269–2277 (1998).
29. Rosenfeld, M.G., Lunyak, V.V. & Glass, C.K. Sensors and signals: a coactivator/co-repressor/epigenetic code for integrating signal-dependent programs of transcriptional response. *Genes Dev.* **20**, 1405–1428 (2006).
30. Reizis, B. & Leder, P. Direct induction of T lymphocyte–specific gene expression by the mammalian Notch signaling pathway. *Genes Dev.* **16**, 295–300 (2002).
31. Yabe, T., Sanagi, T., Schwartz, J.P. & Yamada, H. Pigment epithelium–derived factor induces pro-inflammatory genes in neonatal astrocytes through activation of NF-kappaB and CREB. *Glia* **50**, 223–234 (2005).
32. Yabe, T., Wilson, D. & Schwartz, J.P. NFkappaB activation is required for the neuroprotective effects of pigment epithelium–derived factor (PEDF) on cerebellar granule neurons. *J. Biol. Chem.* **276**, 43313–43319 (2001).
33. Denis-Donini, S., Caprini, A., Frassoni, C. & Grilli, M. Members of the NF-kappaB family expressed in zones of active neurogenesis in the postnatal and adult mouse brain. *Brain Res. Dev. Brain Res.* **154**, 81–89 (2005).
34. Chen, L.F. & Greene, W.C. Shaping the nuclear action of NF-kappaB. *Nat. Rev. Mol. Cell Bio.* **5**, 392–401 (2004).
35. DiDonato, J. *et al.* Mapping of the inducible IkappaB phosphorylation sites that signal its ubiquitination and degradation. *Mol. Cell. Biol.* **16**, 1295–1304 (1996).
36. Harhaj, E.W. & Sun, S.C. Regulation of RelA subcellular localization by a putative nuclear export signal and p50. *Mol. Cell. Biol.* **19**, 7088–7095 (1999).
37. Carlén, M. *et al.* Forebrain ependymal cells are Notch-dependent and generate neuroblasts and astrocytes after stroke. *Nat. Neurosci.* **12**, 259–267 (2009).
38. Cai, J., Jiang, W.G., Grant, M.B. & Boulton, M. Pigment epithelium–derived factor inhibits angiogenesis via regulated intracellular proteolysis of vascular endothelial growth factor receptor 1. *J. Biol. Chem.* **281**, 3604–3613 (2006).
39. Doetsch, F., Petreanu, L., Caille, I., Garcia-Verdugo, J.M. & Alvarez-Buylla, A. EGF converts transit-amplifying neurogenic precursors in the adult brain into multipotent stem cells. *Neuron* **36**, 1021–1034 (2002).
40. Ciccolini, F., Mandl, C., Holzl-Wenig, G., Kehlenbach, A. & Hellwig, A. Prospective isolation of late development multipotent precursors whose migration is promoted by EGFR. *Dev. Biol.* **284**, 112–125 (2005).
41. Yoon, K. & Gaiano, N. Notch signaling in the mammalian central nervous system: insights from mouse mutants. *Nat. Neurosci.* **8**, 709–715 (2005).
42. Sang, L., Coller, H.A. & Roberts, J.M. Control of the reversibility of cellular quiescence by the transcriptional repressor HES1. *Science* **321**, 1095–1100 (2008).
43. Chung, C. *et al.* Anti-angiogenic pigment epithelium-derived factor regulates hepatocyte triglyceride content through adipose triglyceride lipase (ATGL). *J. Hepatol.* **48**, 471–478 (2008).
44. Ang, H.L. & Tergaonkar, V. Notch and NFkappaB Signaling pathways: do they collaborate in normal vertebrate brain development and function? *Bioessays* **29**, 1039–1047 (2007).
45. Espinosa, L., Santos, S., Ingles-Esteve, J., Munoz-Canoves, P. & Bigas, A. p65-NFkappaB synergizes with Notch to activate transcription by triggering cytoplasmic translocation of the nuclear receptor corepressor N-CoR. *J. Cell Sci.* **115**, 1295–1303 (2002).
46. Givogri, M.I. *et al.* Notch signaling in astrocytes and neuroblasts of the adult subventricular zone in health and after cortical injury. *Dev. Neurosci.* **28**, 81–91 (2006).
47. Hsieh, J. & Gage, F.H. Chromatin remodeling in neural development and plasticity. *Curr. Opin. Cell Biol.* **17**, 664–671 (2005).
48. Baek, S.H. *et al.* Exchange of N-CoR co-repressor and Tip60 coactivator complexes links gene expression by NF-kappaB and beta-amyloid precursor protein. *Cell* **110**, 55–67 (2002).

ONLINE METHODS

Mice, immunohistochemistry and *in vivo* infusions. Experiments were performed in TNR mice obtained from the Jackson Laboratories or in CD1 mice (Charles River Labs). Housing of mice and all experiments were carried out according to European Union 86/609/EEC and Spanish RD-1201/2005 guidelines, following protocols approved by the ethics committee of the Universidad de Valencia. Both 7 day infusions into the lateral ventricle of adult mice and BrdU administration regimes have been previously detailed[9,49]. For 24-h infusions, 2-month-old TNR mice received a total of 1.5 μg of PEDF (Biovendor). For primary antibodies, we used rabbit antibodies to N-CoR (1:1, Abcam), GFAP (1:600, Dako), BrdU (1:1500, Megabase Research), EGFP (1:200, Molecular Probes), GLAST (1:1,000, Tocris), S100β (1:200, Dako), activated (cleaved) Notch1 (1:100, Abcam) and Ki67 (1:100, Abcam), mouse antibodies to GFAP (1:500, Sigma), BrdU (1:300, Dako) and Mash-1 (1:100, BD Biosciences), goat antibodies to Sox2 (1:40, R&D Systems) and GFP (1:200, Rockland), guinea pig antibody to GLAST (1:1,000, Chemicon), and sheep antibody to EGFR (1:100, Upstate). For N-CoR immunodetection specifically, 30-μm-thick vibratome and 7-μm-thick paraffin sections were boiled in 10 mM sodium citrate buffer (pH 6.0) for 30 min for antigen retrieval, rinsed twice in 0.1 M phosphate buffer, blocked in 0.1 M phosphate buffer with 10% horse serum (vol/vol, Gibco) and 0.3% Triton X-100 (vol/vol) for 1 h, and incubated with primary antibodies overnight, followed by incubation with biotinylated horse antibody to rabbit (1:200, Vector) and Cy3-conjugated streptavidin (1:200, Jackson Immunochemicals). EGFP expression in TNR mice sections was measured using Leyca Microsystems Confocal Software. The levels of immunofluorescence in each EGFP-positive cell was measured as mean pixel density above background (60 mean pixels; $EGFP^{hi}$ cells, ≥165; $EGFP^{lo}$ cells, 30–165; EGFP-negative cells, ≤30).

Neural stem cell culture, *in vitro* assays and immunofluorescence. Methods for NSC isolation and culture and neurosphere formation analysis have been previously described in detail[49]. We used PEDF (50–100 ng ml^{-1}) from either Bioproducts MD (human recombinant produced in *E. coli*) or from Biovendor (human recombinant produced in HEK cells) with identical results. Jagged1 (2 μg ml^{-1}) and the inhibitors L-685.458 (1 μM) and BAY-11-7082 (0.5 μM) were all from Calbiochem. PEDF and Jagged 1 were added to the medium at the moment of seeding. Inhibitors were added to the medium 1 h before the addition of PEDF. Neurospheres obtained from the SEZ of 2–3-month-old TNR hemizygous mice (Jackson Laboratories) were mechanically dissociated to a single-cell suspension and separated into $EGFP^{hi}$, $EGFP^{lo}$ and EGFP-negative cells by FACS using a MoFlo sorter (Dako). Autofluorescence levels were determined by comparing EGFP intensity with the background fluorescence of a wild-type culture; cells in this range were retrieved as being EGFP negative. The brightest 5–10% of the EGFP-positive cells were collected as $EGFP^{hi}$ and the dimmest 10–20% of the cells were recovered as $EGFP^{lo}$. Cells were seeded at 2.5 cells per μl (low density) or at 1 cell per well in p96 plates (clonal). Clones generated from these FACS-sorted cells were considered to be primary neurospheres in terms of PEDF treatment. Cell apoptosis and viability and the numbers of single viable cells and incipient neurospheres were determined at 24, 48 and 72 h after plating, as previously described[9]. For cell-pair analyses, single cells were seeded and fixed after 24 h with 4% paraformaldehyde (wt/vol) in 0.1M phosphate buffer (pH 7.4). Cell pairs were visually inspected to ensure that they were the results of cell division and at least 50–55 cell pairs were counted in each condition per experiment. Differentiation was analyzed by seeding individual passage 2–3 neurospheres of similar sizes, collected one at a time using a pipette, in Matrigel-coated 96-well plates for 7 d *in vitro* (2 d in neurosphere medium without EGF and another 5 d in 2% fetal bovine serum, vol/vol) before fixation in 4% paraformaldehyde in phosphate buffer and immunocytochemical staining. No less than 50 clones were analyzed for each condition and experiment. Methods for immunofluorescence in proliferating and differentiating neurosphere cultures and in isolated cells have been previously described[49]. For primary antibodies, we used rabbit antibodies to NICD (1:150, Abcam), p65 (1:150, Santa Cruz) and GFAP (1:300, Dako), mouse antibodies to O4 (1:2, Developmental Studies Hybridoma Bank) and βIII-tubulin (1:300, Covance), goat antibody to N-CoR (1:50, Santa Cruz), and sheep antibody to EGFR (1:100, Upstate).

Cell transduction and luciferase assays. We electroporated 2–4 μg of DNA of each of the following constructs using a Nucleofector (II) (Amaxa Biosystems): *HA–Ncor1-C′* (amino acids 1,501–2,300), $I\kappa B\alpha_{32-36}$, *EGFP*, *p65ΔTA*, *p65ΔNES*, *Ncor1*, *Su(H)DBM*, *NotchIC-IRES-GFP*, *Hes1-luc*, *HesΔAB-luc*, *4xwtCBF1-luc*, *4xmutCBF1-luc*, *2xκB-luc* and *Egfr-luc*. In reporter assays with firefly luciferase-based constructs, 50 ng of a *Renilla* luciferase construct was used as an internal control. After 24–36 h, transduced cells (passage 4–6) were dissociated, plated in the presence or absence of PEDF (alone or after a 1-h pre-treatment with inhibitor) and cultured for 24 h before being harvested for analysis. Efficiency was around 80% in all cases. The retrovirus preparation for NotchIC overexpression and NSC infection were performed as described[17]; the neurospheres were mechanically dissociated and transduced cells were isolated by FACS using a MoFlo sorter (Dako). Dissociated transduced cells were plated at 5 cells per μl, treated as described above and cultured for 24 h before harvesting. Luciferase activity was measured in cell lysates using the Dual Luciferase Assay System (Promega) and promoter activity was defined as the ratio between the firefly and *Renilla* luciferase activities.

Co-immunoprecipitation and immunoblot. Isolated cells from passage 4–6 neurospheres were treated with PEDF for 24 h before collecting the cells. For western blot, neurospheres were rinsed in phosphate-buffered saline (PBS), incubated in lysis buffer (20 mM PBS, 150 mM NaCl, 5 mM EDTA, 1% Triton X-100, 1 mM sodium orthovanadate, 1 mM NaF, 1 mM PMSF and 1× Complete (Roche)) for 15 min and centrifuged at 20,000 *g* for 15 min at 4 °C. For preparation of nuclear and cytoplasmic fractions, cells were lysed in cytoplasmic extraction buffer containing 10 mM Tris-HCl (pH 7.6), 1.5 mM $MgCl_2$, 10 mM KCl, 0.5 mM EDTA, 1 mM DTT, 1 mM sodium orthovanadate, 1 mM NaF, 1 mM PMSF and 1× Complete mix (Roche) for 20 min on ice and passed 40 times through a G25 needle. The mix was centrifuged at 1,000 *g* for 15 min and the supernatant containing the cytoplasmic extract was kept. The pellet containing the nuclear cell fraction was resuspended in lysis buffer consisting of 50 mM Tris (pH 8.0), 10 mM EDTA (pH 8.0), 1% SDS (wt/vol), 1 mM PMSF and 1× Complete mix (Roche), incubated for 10 min on ice, and sonicated three times for 30 s (Bioruptor). We used 500–750 μg of protein extract and saved one-tenth of the total volume for input. For co-immunoprecipitation, supernatant was diluted by adding 16.7 mM Tris (pH 8.0), 1.2 mM EDTA (pH 8.0), 1.1% Triton X-100, 90 mM NaCl, 0.01% SDS, 1 mM PMSF and 1× Complete (Roche). Immunoprecipitation was performed overnight at 4 °C with 3 μg of antibody to N-CoR (Affinity Bioreagents) or 3 μg of rabbit IgGs (Sigma). After immunoprecipitation, 60 μl of protein A/G sepharose beads (50% slurry) were added and the incubation continued for another 2 h. Beads were centrifuged and washed and the protein was eluted and subjected to immunoblotting with rabbit antibody to p65 (1:300, Santa Cruz). For western blot, we used rabbit antibodies to N-CoR (1:500) and histone 3 (1:500). Samples were subjected to electrophoresis on SDS-polyacrilamide gel followed by transfer to a nitrocellulose membrane. Membranes were blocked 1 h with 5% nonfat dry milk (wt/vol) and incubated with primary antibodies followed by incubation with horseradish peroxidase–conjugated appropriate secondary antibodies. Western blots were developed using ECL reagents (Amersham) according to supplier recommendations.

ChIP. After PEDF treatment for 24 h, cells (passage 4–8 neurospheres) were cross-linked with 1% formaldehyde (vol/vol) at 20–25 °C for 10 min. Glycine was added to a final concentration of 125 mM to stop cross-linking. Cells were rinsed twice with cold PBS and incubated for 10 min at 4 °C in low-salt washing buffer (10 mM Tris (pH 8.0), 1 mM EDTA (pH 8.0), 0.5 mM EGTA (pH 8.0), 0.25% Triton X-100, 1 mM PMSF and 1× Complete (Roche)). After centrifugation at 1,300*g*, the pellet was resuspended in high-salt washing buffer (10 mM Tris (pH 8.0), 1 mM EDTA (pH 8.0), 0.5 mM EGTA (pH 8.0), 0.2 M NaCl, 1 mM PMSF and 1× Complete (Roche)) and incubated for 10 min at 4 °C. Nuclei were resuspended in 1% SDS lysis buffer and chromatin was sonicated to obtain DNA fragments around 500 base pairs. One-tenth of the total volume was saved as a total input DNA control. Lysates were precleared by incubation with 50 μl of Protein A–sepharose (50% slurry preblocked with salmon sperm DNA, yeast tRNA and BSA) for 1 h. Immunoprecipitation was performed overnight at 4 °C with 5 μg of rabbit antibody to N-CoR (Santa Cruz), 6 μg of rabbit antibody to CBF1 (Santa Cruz), 3 μg of rabbit antibody to NICD (Abcam), 5–6 of μg nonrelated rabbit antibody (Dako) and 3 μg of nonrelated rabbit serum. After immunoprecipitation, 60 μl of preblocked Protein A–sepharose (50% slurry) were added and the

incubation continued for another 4 h. Precipitates were thoroughly washed and extracted twice in 1% SDS and 0.1 M $NaHC0_3$ in TE buffer (10 mM Tris-HCl (pH 8.0), 0.1 mM EDTA). Elutes were incubated at 65 °C overnight to reverse cross-linking, followed by 1 h incubation at 50 °C with 10 μM EDTA, 40 μM Tris-HCl (pH 6.8) and 20 μg of proteinase K (Roche). DNA fragments were recovered by Qiaquick PCR purification kit (Qiagen). For primers, we used Hes1 −176 (5′-GCC GCC AGA CCT TGT GCC TA-3′), Hes +113 (5′-CCA GAT CCT GTG TGA TCC GCA-3′), Egfr −580 (5′-TTC TTT CAG AGA CAT GGA GGG TTC-3′), Egfr −254 (5′-GAA GTC CAG CCA ATC TAT GCC AG-3′), Egfr −109 (5′-TGC CTG CTT TCG ATC CTC-3′), Egfr +224 (5′-AAT CCG AGA CAG ACG GAG-3′), Gfap −265 (5′-GAC TAA GCT GTT CCC TCG GC-3′), Gfap −147 5′-TGA GGT CAC TGT ACC CAG AG-3′), Gfap −2,388 (5′-TGA GCA ACT ACT AGA TCC TTG G-3′), Gfap −2,026 5′-TCT GCC TCT GGT GAC TTT TC-3′), Ptcra −389 (5′-GTA GAG CGA AGG AAC TAG GC-3′) and Ptcra −150 (5′-CAC CCT CTC ATA ACC TTC-3′).

RNA isolation and reverse transcription–PCR analysis. Total RNA was isolated using RNeasy MicroKit (Qiagen) and 1 μg of total RNA was used to synthesize cDNA using random primers and reverse transcriptase (SuperScript II RT, Gibco, Invitrogen). For PCR analysis, 1 μl of cDNA was used as the template in a reaction volume of 20 μl containing 0.25 mM dNTPS (Eppendorf), 0.25 μM primers (Isogen) and 1 U of Taq DNA polymerase (Promega). Transcript levels were quantified by densitometric analysis of reverse transcription–PCR bands in ethidium bromide–stained electrophoresis gels and normalized to β-actin levels. For primers, we used β-actin (forward, 5′-CCG GGA CCT GAC AGA CTA CCT-3′; reverse, 5′-GCC ATC TCC TGC TCG AAG TCT A-3′) and Gfap (forward, 5′-CTC TAG TAC TGC TGC ATG-3′; reverse, 5′-TGT GAG CGT ACT TCT ATG-3′).

Statistical analyses. Analyses of significant differences between means were performed using two-tailed Student's *t* tests. The arcsen transformation for normalization was applied to relative values (fold-change and percentage). In each case, *n* indicates the number of independent cultures or mice used. In all cases, $P < 0.05$ denoted statistical significance.

49. Ferrón, S.R. *et al.* A combined *ex/in vivo* assay to detect effects of exogenously added factors in neural stem cells. *Nat. Protoc.* **2**, 849–859 (2007).

doi:10.1038/nn.2437